UNCLASSIFIED

SECURITY CLASSIFICATION OF THIS PAGE (When Data Entered)

REPORT DOCUMENTATION PAGE		READ INSTRUCTIONS BEFORE COMPLETING FORM
1. REPORT NUMBER	2. GOVT ACCESSION NO.	3. RECIPIENT'S CATALOG NUMBER
4. TITLE (and Subtitle) PREDICTION METHODS FOR THE UNSTEADY TRANSONIC FLOW THROUGH A CASCADE		5. TYPE OF REPORT & PERIOD COVERED FINAL REPORT 6. PERFORMING ORG. REPORT NUMBER NEAR TR 306
7. AUTHOR(s) David Nixon		8. CONTRACT OR GRANT NUMBER(s) N00019-82-C-0288
9. PERFORMING ORGANIZATION NAME AND ADDRESS Nielsen Engineering & Research, Inc. 510 Clyde Avenue Mountain View, CA 94043		10. PROGRAM ELEMENT, PROJECT, TASK AREA & WORK UNIT NUMBERS
11. CONTROLLING OFFICE NAME AND ADDRESS Department of the Navy Naval Air Systems Command Washington, D.C. 20361		12. REPORT DATE July 1983 13. NUMBER OF PAGES 47
14. MONITORING AGENCY NAME & ADDRESS (if different from Controlling Office)		15. SECURITY CLASS. (of this report) UNCLASSIFIED 15a. DECLASSIFICATION/DOWNGRADING SCHEDULE

16. DISTRIBUTION STATEMENT (of this Report)

Approved for Public Release, Distribution Unlimited.

17. DISTRIBUTION STATEMENT (of the abstract entered in Block 20, if different from Report)

18. SUPPLEMENTARY NOTES

19. KEY WORDS (Continue on reverse side if necessary and identify by block number)

Transonic Flow
Unsteady Flow
Cascade Flow

20. ABSTRACT (Continue on reverse side if necessary and identify by block number)

The high frequency cascade code developed in a previous contract for unstaggered cascade has been modified to use a better algorithm. Further developments include the derivation of the mesh and algorithm to treat staggered cascades and the testing of the cascade indicial theory of Nixon which promises considerable reductions in computer cost. The steady flow part of the staggered algorithm works but the unsteady part is not yet operational.

(please turn over)

DD FORM 1 JAN 73 1473 EDITION OF 1 NOV 65 IS OBSOLETE

UNCLASSIFIED

SECURITY CLASSIFICATION OF THIS PAGE (When Data Entered)

20. Several examples of unsteady transonic flows for the unstaggered cascade are given and also results of the indicial theory.

COPY NO. 17

PREDICTION METHODS FOR THE UNSTEADY TRANSONIC FLOW THROUGH A CASCADE

by

David Nixon

~~NEAR~~ TR 306
July 1983

Prepared Under Contract No. N00019-82-C-0288

for

NAVAL AIR SYSTEMS COMMAND
Washington, D.C. 20361

by

NIELSEN ENGINEERING & RESEARCH, INC.
510 Clyde Avenue, Mountain View, CA 94043
Telephone (415) 968-9457

TABLE OF CONTENTS

1. INTRODUCTION

An important problem in turbomachinery is the prediction of the flutter boundaries of the compressor and, in order to compute these boundaries, the unsteady aerodynamic forces need to be understood. The aerodynamic causes of flutter in a compressor can be very complex, for example, the interaction between the flows induced by the rotor and stator, but an important class of flutter is caused by a relatively simple aerodynamic flow due to vibration of the blades on a given compressor row without the added complexity of exterior interactions. This latter problem is the simplest unsteady aerodynamic phenomenon of interest. In a compressor the oncoming velocity varies along the compressor blade, increasing from subsonic speeds at the hub to perhaps transonic speeds at the tip; it is the prediction of unsteady transonic flow in a compressor that is the most difficult. This proposal is concerned with the prediction of flutter in a vibrating compressor row when the flow is transonic.

Because of the general complexity of even the simple compressor row flow, several simplifications must be made in order to obtain a tractable problem. The first simplification is to assume that radial velocities are small relative to axial velocities and unwrap the compressor row to form a two-dimensional cascade. The second simplification is to assume, in the first instance, that viscous effects are negligible and that any shock waves present are sufficiently weak such that potential theory can be used. In certain circumstances the potential equation model can be simplified further to yield the unsteady, high frequency transonic small disturbance (TSD) equation. This is the simplest equation that will represent the dominant feature of the flow. It can be noted that viscous effects can be represented by the inclusion of a boundary layer model.

A major problem with potential theory is that it is not valid (Ref. 1) when shock waves are present and, as a consequence, that shock locations are not predicted adequately for medium to strong shock strengths, although the agreement for flows with weak shocks is acceptable. This disadvantage of the potential formulation can be overcome by modifying the theory to give the correct shock jump. This has been done by Nixon (Ref. 2) for the steady small disturbance equation and by Kerlick, Nixon, and Ballhaus (Ref. 3) for the unsteady low frequency equation. A more complete analysis for steady flow (Ref. 4) indicates that such modified equations can essentially duplicate the Euler equations.

Most of the numerical methods for predicting unsteady transonic flow stem from the work of Ballhaus and Goorjian (Ref. 5), who developed an implicit algorithm to solve the low frequency TSD equation for isolated airfoils. An extension of this algorithm to high frequency motion was made by Rizzetta and Chin (Ref. 6). For cascade flows a version of the Rizzetta-Chin algorithm was used by Kerlick and Nixon (Ref. 7) to develop a method for cascade flows for unstaggered cascades. An alternative to the use of the unsteady TSD equation has been considered by Verdon and Caspar (Ref. 8) who use a time linearized perturbation of the full potential equation for staggered and unstaggered cascades in a subsonic flow. The methods of References 5-7 can treat moving shock waves but it is not clear at present whether the time linearized method is capable of such a representation, since it does not possess the essential double-valued character at a shock location.

In a cascade flutter analysis the dominant parameter is the interblade phase angle which can determine the conditions at which the blade will flutter. In a numerical method, such as those discussed earlier, a flutter calculation can involve computing a test case for each value of the interblade phase angle.

This is computationally expensive and, in order to reduce the cost, a technique developed by Nixon (Ref. 9) may be used. This technique, which is based on indicial theory, decouples the cascade problem into a series of elementary problems, which are parametrically related, and only one solution need be computed numerically. This elementary solution consists of a number of blades, all stationary with the exception of one blade which undergoes a step change. Once computed, the full unsteady solution for any frequency and interblade phase angle can be constructed by a judicious superposition.

The present work is concerned with the development of the unsteady transonic flow through a cascade. Earlier work concentrated on unstaggered cascades with the present study concerned with extending the method to treat staggered cascades. These studies are performed under contracts N00018-81-C-0169 and N00019-82-C-0288. In addition to the development of the flow prediction code, the ideas of Reference 9 have been tested to determine whether flutter prediction at transonic speeds is possible without resorting to an expensive series of calculations for a range of interblade phase angles.

The flow prediction code is a development of the Ballhaus-Goorjian (Ref. 5) code to include the high frequency algorithm of Rizzetta and Chin (Ref. 6) and to extend the geometry of the problem from an isolated airfoil to that of a cascade. The present code is limited by computer storage to a 12-blade cascade. The code is composed of two distinct parts, namely a steady flow part which is periodic in a blade-to-blade sense, which is solved by a relaxation algorithm, and an unsteady flow part which uses an alternating direction implicit (ADI) algorithm. The unsteady part of the code requires that the interblade phase angle be specified or, if run in the indicial mode, that a relatively large number of blades (usually seven) be used for the calculation.

At present, the computer code works for unstaggered cascades but the extension to staggered cascades has not been completed.

In order to test the validity of the method of Reference 9, the flow prediction code was run in its indicial mode and the resulting indicial responses used to compute the magnitude and phase lag of lift and pitching moment coefficients. A comparison of values computed by this method and the direct calculation method discussed earlier shows good agreement.

The computation time required to obtain the indicial response for a seven-blade cascade, and to use this data to compute the oscillatory lift and moment coefficients, is approximately 500 cpu seconds on a CDC 7600 computer. This figure is essentially unchanged if a range of interblade phase angles and frequencies are to be computed. The direct computation requires 250 cpu seconds for <u>each</u> interblade phase angle and for <u>each</u> frequency. Hence, in a flutter calculation the method of Reference 9 offers a considerable reduction in computation time.

While it can be stated that the agreement of the present methodology with other available test cases is satisfactory, there are areas that need to be further investigated before the true worth of the technique can be determined. These points are noted in the text.

This report consists of two more or less separate parts, namely the development of an algorithm for the unsteady cascade code and the development of the indicial theory. Although the latter uses the numerical data generated by the unsteady cascade code, it is not tied to this particular program; any suitable computer code can be used to calculate the necessary input.

2. UNSTEADY TRANSONIC CASCADE CODE

2.1 Unstaggered Algorithm

Although a preliminary version of the cascade algorithm has been described in Reference 7, there have been sufficient modifications to the algorithm to warrant a further description.

The basic equation is the high frequency transonic small disturbance (TSD) equation (see Ref. 5):

$$A\phi_{tt} + 2B\phi_{xt} = C\phi_{xx} + \phi_{yy} \tag{1}$$

where:

$$A = \nu^2 M_\infty^2 \delta^{-2/3}$$

$$B = A\nu^{-1}$$

$$C = (1 - M_\infty^2)\delta^{-2/3} - (\gamma + 1)M_\infty^q \phi_x$$

Here ϕ is the perturbation velocity potential, M_∞ is the free stream Mach number, γ is the ratio of specific heats, δ is the thickness parameter and q is the transonic scaling parameter. The quantities x, y, t, ϕ are in the scaled units of Reference 5. The reduced frequency based on chord c is $\nu = \omega c/U_\infty$, where ω is the frequency and U_∞ is the free stream velocity.

Ballhaus and Goorjian (Ref. 5) solve Equation (1) in the case where A = 0, which applies for reduced frequencies less than about 0.2 in the code LTRAN2. The unsteady effects which are of interest, primarily cascade flutter, occur at reduced frequencies (based on blade chord) of about one to ten. Since the Ballhaus-Goorjian algorithm is not designed for these frequencies, high frequency modifications must be made.

Houwink and van der Vooren (Ref. 10) and Hessenius and Goorjian (Ref. 11) solve Equation (1), still with A = 0, but with improvements in the definition of C_p, and the airfoil and wake boundary conditions. Rizzetta and Chin (Ref. 7) solve the

full Equation (1), including the $A\phi_{tt}$ term, with improved boundary conditions. Their algorithm is summarized briefly in the following section.

2.2 Rizzetta-Chin Algorithm

The Ballhaus-Goorjian algorithm has two components, a steady TSD equation solver by either successive line over-relaxation (SLOR) or approximate factorization (AF2) algorithms, and an unsteady solver based on the alternating direction implicit (ADI) algorithm. Only the unsteady solver is modified for high reduced frequencies. The airfoil boundary condition is applied on the split coordinate line at y = 0 (see Fig. 1). The algorithm approximates Equation (1) by finite differences at a time level $t^{n+1/2}$ in order to solve for the velocity potential function ϕ at time level t^{n+1}, given ϕ at time t^n (Ref. 12). For the high frequency equation, Rizzetta and Chin approximate the additional term $A\phi_{tt}$ by a first-order accurate three-point backward difference:

$$\phi_{tt} = \frac{\phi^{n+1} - 2\phi^{n} + \phi^{n-1}}{(\Delta t)^2} + \frac{\Delta t}{2}\,\phi_{ttt}\Big|_{n+1/2} + \theta(\Delta t^2) \qquad (2)$$

The algorithm is divided into an x-sweep and a y-sweep as follows:

x-sweep

$$2B(\Delta t)^{-1}\delta x(\tilde{\phi} - \phi^{n})_{i,j} = D_x f_{i,j} + \phi^{n}_{yy\ i,j} \qquad (3)$$

y-sweep

$$A(\Delta t)^{-2}(\phi^{n+1} - 2\phi^{n} + \phi^{n-1})_{i,j} + 2B(\Delta t)^{-1}\delta_x(\phi^{n+1} - \tilde{\phi})_{i,j} = \frac{1}{2}\,\delta_{yy}(\phi^{n+1} - \phi^{n})_{i,j} \qquad (4)$$

Here, the term $D_x f_{i,j}$ is the nonlinear term defined in Equation (10) of Reference 5 which includes type-dependent differencing by means of a switching operator. The only change from the Ballhaus-Goorjian method is the addition of the $A\phi_{tt}$ term in the y-sweep which is treated in such a way to retain conservation form. In the low-frequency case, this algorithm ensures correct capture of a moving shock wave (Ref. 12). The total algorithm can be readily obtained by eliminating the intermediate variable ϕ, whereby in the subsonic (central differences δ_{xx})

$$A(\Delta t)^{-2}(\phi^{n+1} - 2\phi^n + \phi^{n-1})_{i,j} + 2B(\Delta t)^{-1}(\phi^{n+1} - \phi^n)i,j$$

$$= \frac{C}{2}\,\delta_{xx}(\phi^{n+1} + \phi^n)_{i,j} + \frac{1}{2}\,\delta_{yy}(\phi^{n+1} + \phi^n)_{i,j} + TE \qquad (5)$$

Here, TE represents the truncation error incurred by approximately factorizing the differential operators. For subsonic flow, the truncation error is given by

$$TE = \frac{AC\Delta t}{4B}\,\delta_x^{-1}\delta_{xx}\delta_{tt}\phi - \frac{C\Delta t^2}{8B}\,\delta_x^{-1}\delta_{xx}\delta_{yy}\delta_t\phi \qquad (6)$$

The symbol δ_x^{-1} indicates integration. Equation (6) indicates that the new algorithm is first-order time accurate, whereas the low frequency algorithm is second-order time accurate.

The pressure coefficient, C_p, is given by

$$C_p = -2\delta^{2/3}(\phi_x + \nu\phi_t) \qquad (7)$$

and the airfoil tangency condition is

$$\phi_y(x,0) = f_x + \nu f_t \qquad (8)$$

where $f(x,t)$ represents the airfoil surface. The downstream boundary condition is

$$\phi_x + \nu\phi_t = 0 \qquad (9)$$

and the initial condition

$$\phi_t(0) = h(x,y) \tag{10}$$

Usually $h(x,y)$ is put equal to zero.

The far field boundary condition of Ballhaus and Goorjian, namely $\phi = 0$ (reflective) for the upstream boundary is applied unchanged. This is not really the physically correct boundary condition for a cascade, but the mesh is stretched to some 800 chords away from the airfoil, which should minimize the effect of the boundary condition. This minimum influence of the far field boundaries has been observed in numerical experiments.

The vorticity shed at the trailing edge is represented by a discontinuity $\Gamma(x,t) = \phi(x,+0,t) - \phi(x,-0,t)$ in the perturbation potential across the blade chord line. Following References 6 and 11, this discontinuity is convected downstream with the free stream velocity, thus

$$\Gamma_x + \nu\Gamma_t = 0 \tag{11}$$

This ensures that the pressure is continuous across the wake.

The initial steady flow through the cascade is calculated in the manner described in Reference 7.

The unsteady solution is periodic over the whole cascade of N blades, so the unsteady calculation takes place on a mesh which is an N-fold replica of the steady-state mesh, thus the entire cascade is represented. Again, the blades and wakes are represented by split coordinate lines.

First, the grid is swept in the y-direction from bottom to top with implicit quadridiagonal solvers used on the y-constant lines. The lower surfaces, interblade lines, and the upper surfaces, are solved in turn.

Next, the grid is swept in the x-direction. For the region ahead of the leading edge, periodic boundary conditions are used with a period of the entire grid (N interblade spaces), and the periodic tridiagonal solver is again used. From the leading edge to trailing edge, each x-constant line for each interblade region is solved using a separate tridiagonal inversion with thin airfoil boundary conditions applied at both ends. Aft of the trailing edge, the periodic solver for the entire cascade (N blades) is used, with the upper surface potentials being obtained by adding the corrected circulation propagated back from the trailing edge according to the wake condition, Equation (11).

2.3 Results for Unstaggered Mesh

A series of computations were made for several test cases at both subcritical and supercritical Mach numbers. In Figure 2 is shown the steady flow through an advanced supercritical cascade designed by Sanz (Ref. 13) at a free stream Mach number (M_∞) of 0.692 and a gap/chord ratio (G) of 1.373. The agreement with the results of Sanz is adequate. It should be noted that it proved to be relatively difficult to converge this case.

In Figure 3 the unsteady pressure difference over a flat plate oscillating in bending with reduced frequency (ν) of one and M_∞ = 0.5, G = 1.0, is compared to the results of Verdon and Caspar (Ref. 8). The agreement is good. For a similar case involving torsion, the agreement between the two methods is not as good, as can be seen in Figure 4. The reason for this discrepancy is not clear at present. Figure 5 shows the pressure difference for a NACA0012 section, M_∞ = 0.5, G = 1.0, ν = 1.0 oscillating in torsion. Again, the agreement with the result of Verdon and Caspar is not good.

Figure 6 shows the unsteady pressure difference for a NACA0012 cascade at a supercritical Mach number of 0.75, ν = 1.0, G = 2. Figure 7 shows the unsteady pressure difference

for the Sanz cascade at $M_\infty = 0.707$, $G = 1.373$, $\nu = 1.0$. It can be seen that the presence of shock waves affects the unsteady flow considerably.

A comparison of the magnitude and phase for C_L and C_m for several cascades is shown in Table I.

3. UNSTEADY CASCADE ALGORITHM

In a staggered cascade the natural coordinate system is one in which periodicity can be applied along grid lines. Consequently, if coordinates (ξ,η) are defined as

$$\begin{aligned} x &= \xi + y \sin \theta_s \, \delta^{-1/3} \\ y &= \eta \cos \theta_s \end{aligned} \tag{12}$$

where θ_s is the stagger angle, the TSD equation, Equation (1), can be written as

$$\bar{A}\phi_{tt} + 2\bar{B}\phi_{\xi t} = (\bar{C} + S^2)\phi_{\xi\xi} - 2S_{\xi\eta} + \phi_{\eta\eta} \tag{13}$$

where:

$$\begin{aligned} \bar{A} &= A \cos^2 \theta_s \\ \bar{B} &= B \cos^2 \theta_s \\ \bar{C} &= \delta^{-1/3} \sin \theta_s \end{aligned}$$

The tangency boundary condition is now

$$\phi_\eta(\xi,t) = (f_\xi + \nu f_t) \cos \theta_s + S\phi_\xi \tag{14}$$

Equation (13) is similar to the unstaggered equation, Equation (1), with the exception of the cross-derivative, $-2S\phi_{\xi\eta}$. This term can cause numerical difficulties because of the fact that in the (ξ,η) coordinate system, the domain of dependence in the supersonic zone, defined by the characteristics, is no longer contained in a simple difference stencil, as shown in Figure 8. A solution to this difficulty has been proposed by Rae (Ref. 14)

for steady flow, who used a seven-point formula to represent the cross-derivative. Thus,

$$\phi_{\xi\eta} = (\Delta\xi\Delta\eta)^{-1}(-\phi_{i-1,j+1} + \phi_{i,j+1} + \phi_{i-1,j} - 2\phi_{ij} + \phi_{i,j-1} + \phi_{i+1,j} - \phi_{i+1,j-1}) \qquad (15)$$

In the relaxation scheme, data at the intermediate time level, denoted by $\tilde{\phi}$, is given by

$$(\Delta\eta)^{-2}(\tilde{\phi}_{i,j+1} - 2\tilde{\phi}_{ij} + \tilde{\phi}_{i,j-1}) + \bar{C}(\Delta\xi)^{-2}[\tilde{\phi}_{i-1,j} - 2\tilde{\phi}_{ij} + \phi^{n}_{i+1,j}]$$

$$= S(\Delta\xi\Delta\eta)^{-1}(-\tilde{\phi}_{i-1,j+1} + \tilde{\phi}_{i,j+1} + \tilde{\phi}_{i-1,j} - 2\tilde{\phi}_{ij} + \tilde{\phi}_{i,j-1} + \phi^{n}_{i+1,j} - \phi^{n}_{i+1,j-1})$$

$$- S^{2}(\Delta\xi)^{-2}(\tilde{\phi}_{i-1,j} - 2\tilde{\phi}_{ij} + \phi^{n}_{i+1,j}) \qquad (16)$$

where the superscript n denotes a value at the previous time level. The final result at time n+1 is given by

$$\phi^{n+1}_{ij} = \omega\tilde{\phi}_{ij} + (1-\omega)(\tilde{\phi} - \phi^{n}) \qquad (17)$$

where ω is a relaxation factor. In regions of supersonic flow, the term in square brackets in Equation (16) is upwind differenced. None of the other ξ differences are treated this way since they are due to the ϕ_{yy} term in the original equation, Equation (1).

Some results of using this algorithm are shown in Figure 9, where the steady pressure distribution through a cascade of NACA0012 section blades at $M_{\infty} = 0.75$ and $G = 2$ are shown for various stagger angles. It may be seen that the effects of stagger are significant.

For unsteady flow problems, a difficulty arises in incorporating the seven-point scheme into the alternating direction algorithm (ADI) used in the existing code. The difficulty is

that the ADI algorithm sweeps first in the ξ direction and then in the η direction, therefore at a given time level all of the unknowns in a row must be at the same time. Thus the differencing of the cross-derivative operator $\delta_{\xi\eta}$, where

$$\delta_{\xi\eta}\phi = [(\phi_{i-1,j} + \phi_{i,j+1} - \phi_{ij} - \phi_{i-1,j+1})/(\Delta\xi\Delta\eta)] + [(\phi_{i+1,j} - \phi_{i+1,j-1} + \phi_{i,j-1} - \phi_{ij})/(\Delta\xi\Delta\eta)] \quad (18)$$

must be decomposed into the appropriate time levels. If the first term in square brackets on the right-hand-side of Equation (18) is denoted by $\delta^{NW}_{\xi\eta}\phi$ and the second term by $\delta^{SE}_{\xi\eta}\phi$, then the ADI algorithm is as follows:

ξ-sweep

$$\frac{2\bar{B}}{\Delta t}\delta_\xi(\tilde{\phi}-\phi^n) = \frac{\bar{C}}{2}\delta_{\xi\xi}(\tilde{\phi}+\phi^n) + \delta_{\eta\eta}\phi^n + \frac{S^2}{2}\delta_{\xi\xi}(\tilde{\phi}+\phi^n) - 2S\lambda\delta^{NW}_{\xi\eta}\phi^n - S(1-\lambda)\delta^{SE}_{\xi\eta}(\tilde{\phi}+\phi^n) \quad (19)$$

η-sweep

$$\frac{\bar{A}}{\Delta t^2}(\phi^{n+1} - 2\phi^n + \phi^{n-1}) + \frac{2B}{\Delta t}\delta_\xi(\phi^{n+1} - \tilde{\phi}) = \frac{1}{2}\delta_{\eta\eta}(\phi^{n+1} - \phi^n) - S\lambda\delta^{NW}_{\xi\eta}(\phi^{n+1} - \phi^n) \quad (20)$$

λ is a parameter, which if equal to 1/2, gives a second-order accurate algorithm.

On the upper surface of the blade the cross-derivative term is represented by $\delta^{NW}_{\xi\eta}$ and on the lower surface by $\delta^{SE}_{\xi\eta}$. This leads to a first-order accurate treatment of the boundary conditions.

At the present time the above algorithm does not work; there seems to be a problem with the boundary conditions at the leading and trailing edges of the blade.

4. APPLICATIONS OF THE INDICIAL THEORY

The indicial theory is described in Reference 9, and is given as the Appendix. In brief, if an elementary solution for, say, the lift coefficient $C_{L_o}(t)$ due to a motion by one blade in a cascade of 2N+1 blades with the other blades stationary, the lift coefficient on the blade for the whole cascade moving with a phase lag of σ is

$$C_L(t) = \sum_{i=-N}^{N} C_{L_i}(t-i\sigma) \tag{21}$$

where $C_{L_i}(t)$ is the lift on the ith blade in the elementary solution. If the variable blade undergoes a step change in the elementary solution of ε, then Equation (21) gives an indicial response $C_{L_\varepsilon}(t)$, where

$$C_{L_\varepsilon}(t) = (C_L(t) - C_{L_o})/\varepsilon \tag{22}$$

and any time-dependent motion can be constructed using the indicial theory of Reference 15. Thus, for an oscillatory cascade the lift coefficient is given by

$$C_L(t) = C_{L_o} + C_{L_\varepsilon}(t)\varepsilon(o) + \int_o^t C_{L_\varepsilon}(\tau)\,\frac{d\varepsilon(t-\tau)}{dt}\,d\tau \tag{23}$$

where $\varepsilon(t)$ is a specified motion. If the motion is harmonic with reduced frequency ν, the real and imaginary parts of C_L are given by

$$C_L^R = C_{L_\varepsilon}(\infty) - \nu\int_o^\infty \Delta C_{L_\varepsilon}(\tau)\,\sin\,\nu\tau d\tau \tag{24a}$$

$$C_L^I = C - \nu\int_o^\infty \Delta C_{L_\varepsilon}(\tau)\,\cos\,\nu\tau d\tau \tag{24b}$$

where

$$\Delta C_{L_\varepsilon}(\tau) = C_{L_\varepsilon}(\infty) - C_{L_\varepsilon}(\tau) \qquad (25)$$

A similar relation appears for the moment coefficient, C_M^R, C_M^I.

Turbomachinery flutter will occur in simple torsion if C_M^I is positive and for simple bending if C_L^I is positive.

4.1 Results

The above theory was used to compute lift and moment coefficients for cascades with variations of interblade phase angle, frequency and Mach number. The elementary solutions necessary for the evaluation of the sum in Equation (21) are computed using the unstaggered cascade code described earlier.

In order to test the method, the indicial theory was used to compute the magnitude and phase angle for a cascade of NACA0012 sections in torsion at $\nu = 1.0$, $G = 2$ and at $M_\infty = 0.5$ and 0.75. These were compared to directly computed results, and this is shown in Table 2.

The variation of the real and imaginary moment coefficients with interblade phase angle for a NACA0012 cascade at $M_\infty = 0.75$ and a flat plate cascade at $M_\infty = 0.5$ are shown in Figure 10. It can be seen that there is a considerable difference between the results.

Figure 11 shows the variation of real and imaginary moment coefficients for a NACA0012 cascade at $M_\infty = 0.75$, $G = 2$ for various frequencies. It can be seen that the variation with frequency is considerable and that at $\nu = 1.2$ the imaginary part of the pitching moment becomes positive, indicating a tendency to flutter.

It proved difficult to obtain indicial responses to the supercritical cascade. The reason is not clear, although it is possible that one of the nonunique solutions described by Steinhoff and Jameson (Ref. 16) may be present.

The computation time required to obtain the indicial response for a seven-blade cascade, and to use this data to compute the oscillatory lift and moment coefficients, is approximately 500 cpu seconds on a CDC 7600 computer. This figure is essentially unchanged if a range of interblade phase angles and frequencies are to be computed. The direct computation requires 250 cpu seconds for each interblade phase angle and for each frequency. Hence, in a flutter calculation the method of Reference 9 offers a considerable reduction in computation time.

5. CONCLUDING REMARKS

A computer code to calculate the unsteady transonic flow through a cascade has been developed for unstaggered cascades. Although an algorithm for staggered cascades has been derived, it has not yet resulted in a workable computer code. Results for the unstaggered case agree quite well with other solutions for subsonic flows, but there are some discrepancies that should be explained in the future.

This computer code has been used to generate input data for testing the cascade indicial method of Reference 9. The results look encouraging, but more testing is desirable. The indicial method promises greatly reduced computer time for cascade flutter calculations.

REFERENCES

1. Nixon, D. and Klopfer, G. H.: Some Remarks on Transonic Potential Flow Theory. Nielsen Engineering & Research, Inc. Paper 155 (to be published in Journal of Applied Mechanics), 1982.

2. Nixon, D.: Transonic Small Disturbance Theory with Strong Shock Waves. AIAA Journal, Vol. 18, No. 6, 1980.

3. Kerlick, G. D., Nixon, D., Ballhaus, W. F.: Unsteady Transonic Small Disturbance Theory with Strong Shock Waves. Nielsen Engineering & Research, Inc. TR 230 (also AIAA Paper 82-0159), 1980.

4. Klopfer, G. H. and Nixon, D.: Non Isentropic Potential Formulation for Potential Flows. Nielsen Engineering & Research, Inc. Paper 156 (also AIAA Paper 83-0375), 1982.

5. Ballhaus, W. F. and Goorjian, P. M.: Implicit Finite-Difference Computations of Unsteady Transonic Flows About Airfoils Including the Effect of Irregular Shock Motions. AIAA Journal, Vol. 15, No. 12, Dec. 1977, pp. 1728-1735.

6. Rizzetta, D. P. and Chin, W. C.: Effect of Frequency in Unsteady Transonic Flow. AIAA Journal, Vol. 17, No. 7, 1979.

7. Nixon, D. and Kerlick, G. D.: A High-Frequency Transonic Small Disturbance Code for Unsteady Flows in a Cascade. Nielsen Engineering & Research, Inc. TR 277 (also AIAA Paper 82-0955), Sep. 1982.

8. Verdon, J. M. and Caspar, J. R.: Subsonic Flow Past an Oscillating Cascade with Finite Mean Flow Deflection. AIAA Journal, Vol. 18, No. 5, 1980.

9. Nixon, D.: Computation of Unsteady Transonic Cascade Flows. AIAA Journal, Vol. 21, No. 5, 1983.

10. Houwink, R. and van der Vooren, J.: Results of an Improved Version of LTRAN2 for Computing Unsteady Airloads on Airfoils Oscillating in Transonic Flow. AIAA Paper 79-1553, AIAA 12th Fluid and Plasma Dynamics Conference, Williamsbrg, VA, Jul. 23-25, 1979.

11. Hessenius, K. A. and Goorjian, P. M.: A Validation of LTRAN2 with High Frequency Extensions by Comparisons with Experimental Measurements of Unsteady Transonic Flows. NASA TM-81307, Jul. 1981.

12. Ballhaus, W. F. and Steger, J. L.: Implicit Approximate-Factorization Schemes for the Low-Frequency Transonic Equation. NASA TM X-73982, Nov. 1975.

13. Sanz, J.: Private Communication, 1981.

14. Rae, W. J.: Calculations of Three Dimensional Transonic Compressor Flowfields by a Relaxation Method. Journal of Energy, Vol. 1, No. 5, pp. 284-296.

15. Ballhaus, W. F. and Goorjian, P. M.: Computation of Unsteady Transonic Flows by the Indicial Method. AIAA Journal, Vol. 16, No. 2, pp. 117-224, 1978.

16. Steinhoff, J. and Jameson, A.: Multiple Solutions of the Transonic Potential Flow Equation, AIAA Journal, Vol. 20, No. 11, pp. 1521-1525.

TABLE 1.- C_L AND C_M FOR VARIOUS CASCADES

Section	M_∞	G	ν	$\lvert C_L \rvert$	ϕ_L°	$\lvert C_M \rvert$	ϕ_M°
Flat Plate	0.7	2.0	1.0	8.61	-26.2	2.068	-63.3
NACA 0012	0.75	2.0	1.0	3.17	-57.5	1.648	-231.4
Sanz	0.707	1.373	1.0	2.90	-51.6	1.132	-221.5

TABLE 2.- COMPARISON OF MAGNITUDES AND PHASE ANGLES OF LIFT AND MOMENT COEFFICIENTS FOR NACA 0012 SECTION OF INTERBLADE PHASE ANGLE OF 180°

M_∞	Method of Ref. 1				Direct Calculation			
	$\lvert C_L \rvert$	ϕ_L°	$\lvert C_M \rvert$	ϕ_M°	$\lvert C_L \rvert$	ϕ_L°	$\lvert C_M \rvert$	ϕ_M°
0.50	6.840	-13.2	2.040	-173.3	6.776	- 9.4	1.968	-169.7
0.75	3.428	-57.7	1.812	-227.6	3.170	-57.5	1.647	-231.4

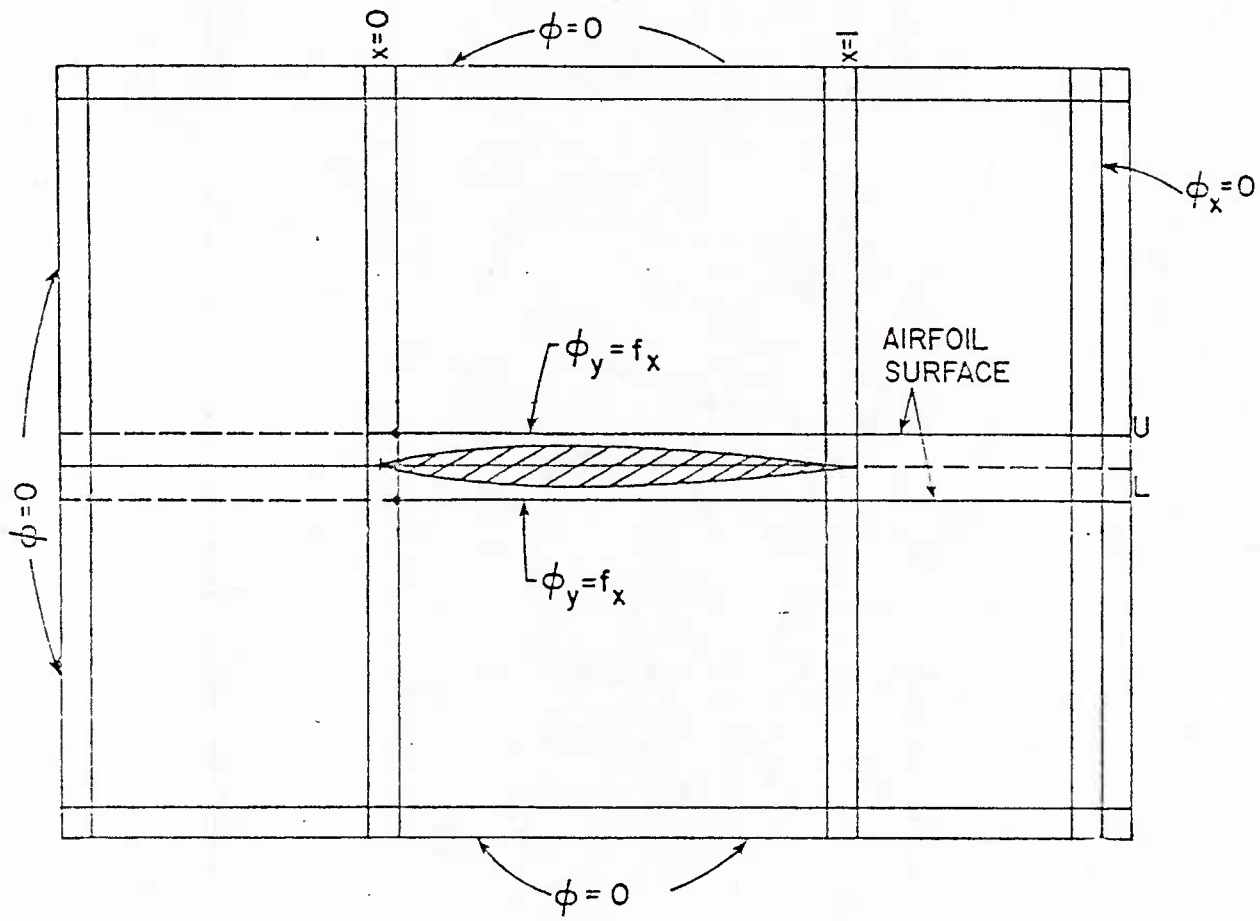

Figure 1. LTRAN2 mesh schematic and boundary conditions for an isolated airfoil.

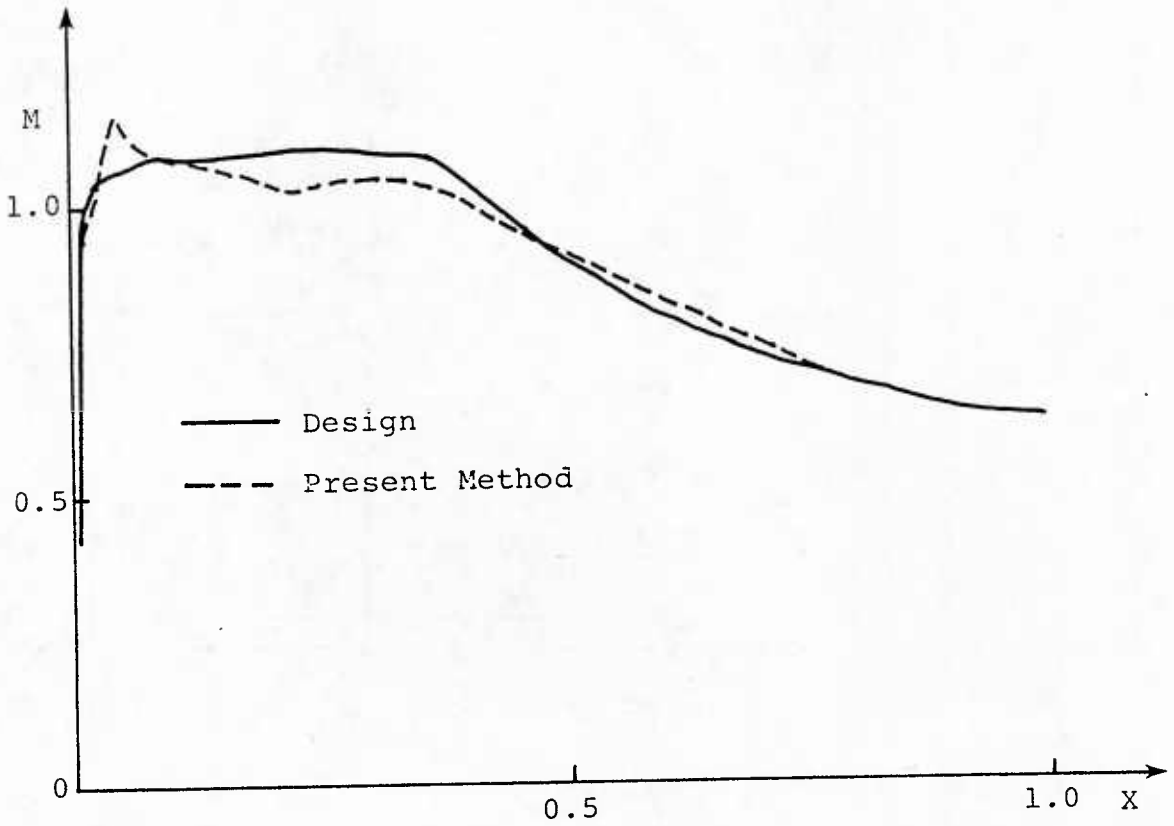

Figure 2.- Steady pressure distribution around a supercritical blade cascade; $M_\infty = 0.692$, $G = 1.372$.

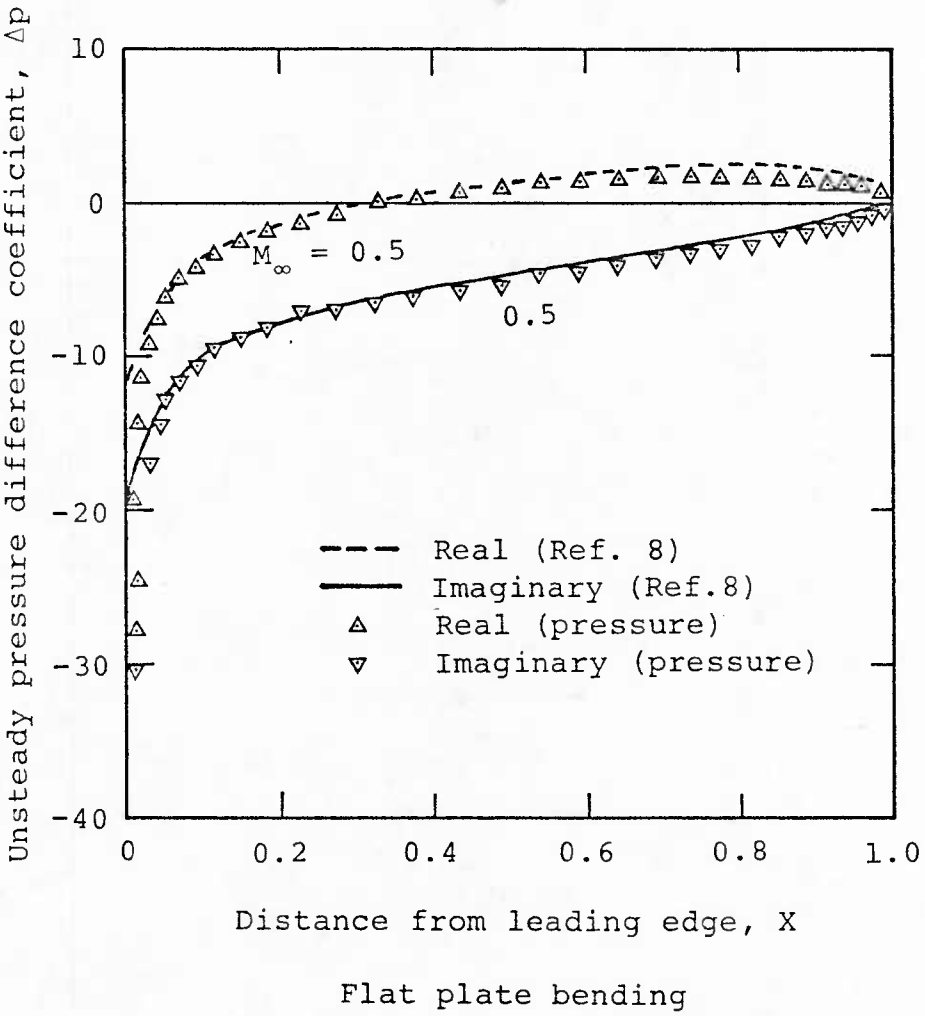

Figure 3.- Pressure distribution for a flat plate oscillating in bending; $M_\infty = 0.5$, $\nu = 1.0$.

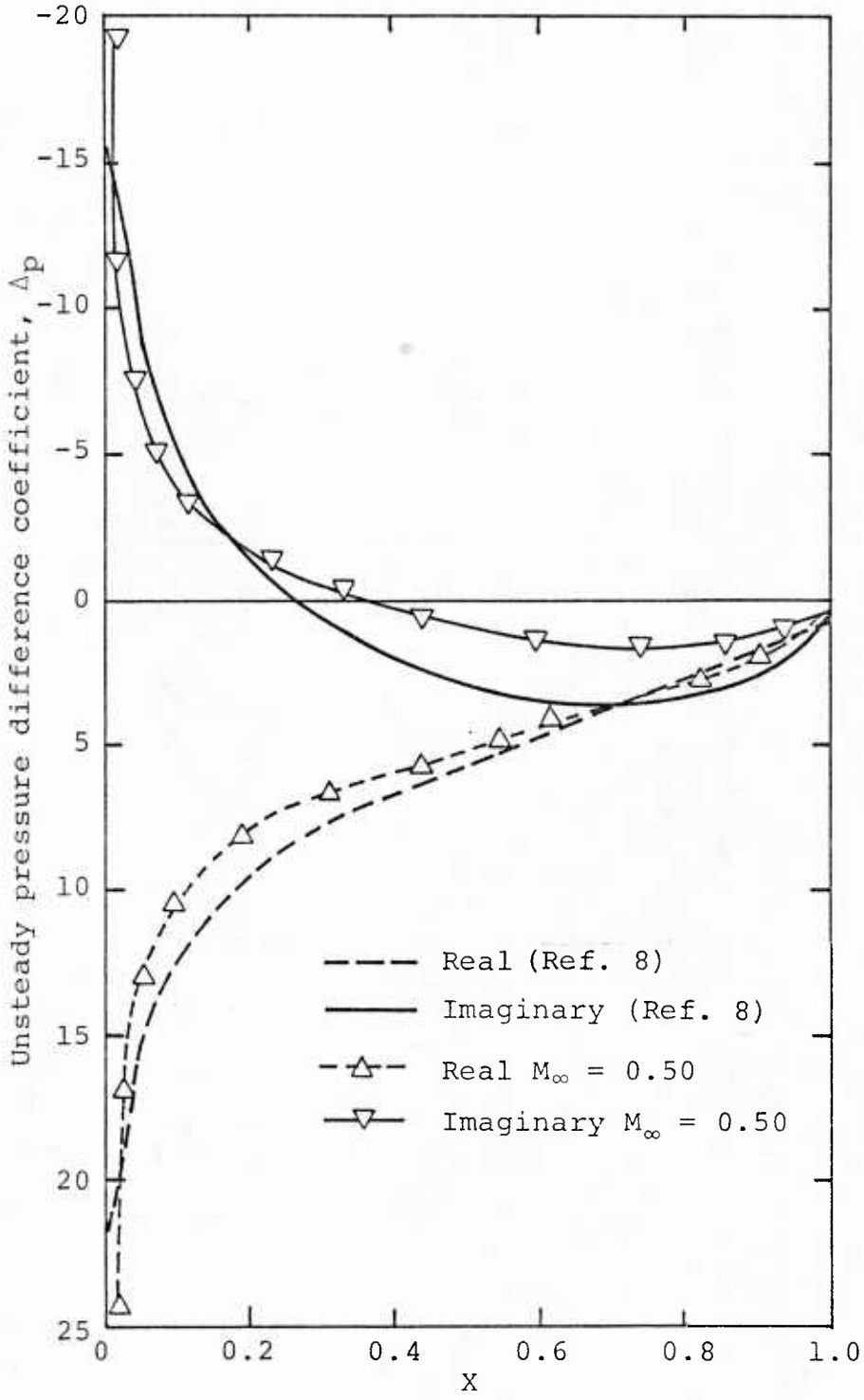

Figure 4.- Unsteady pressure distribution around a flat plate in torsion; $M_\infty = 0.5$, $G = 1.0$, $\nu = 1.0$.

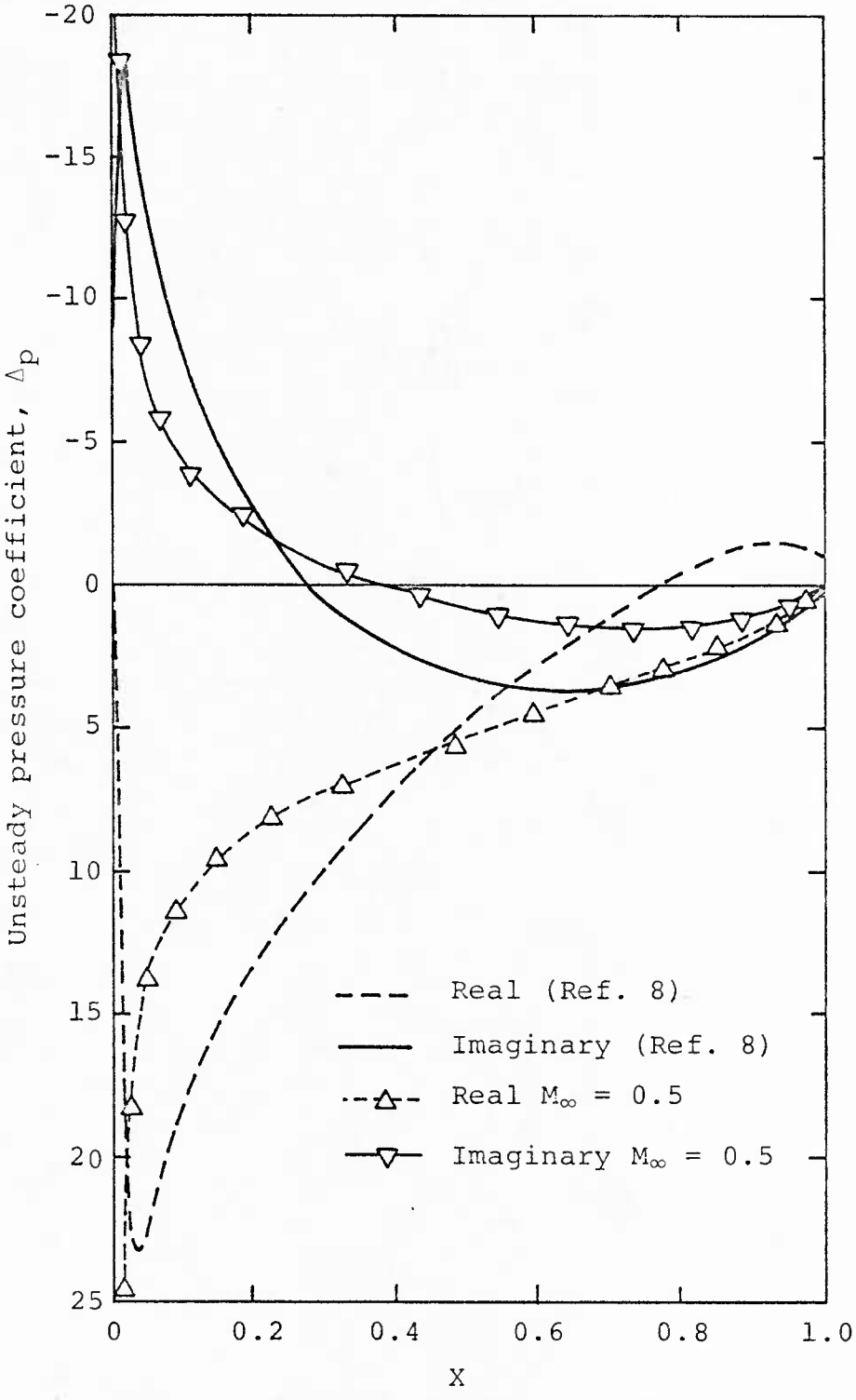

Figure 5.- Unsteady pressure distribution around a cascade of NACA 0012 blade in torsion: $M_\infty = 0.5$, $G = 1.0$, $\nu = 1.0$.

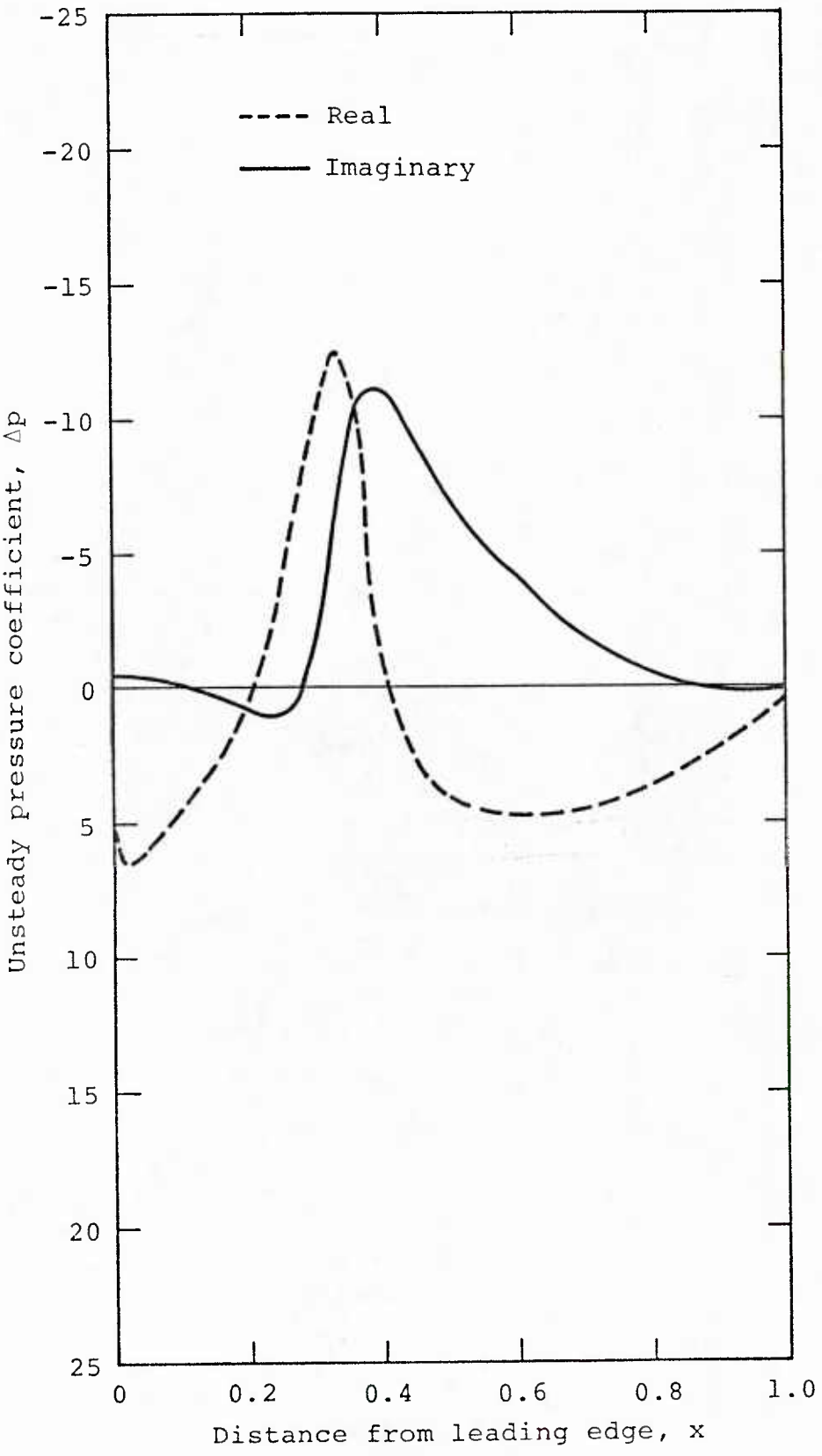

Figure 6.- Pressure distribution for a NACA 0012 blade oscillating in torsion; $M_\infty = 0.75$, $\nu = 1.0$.

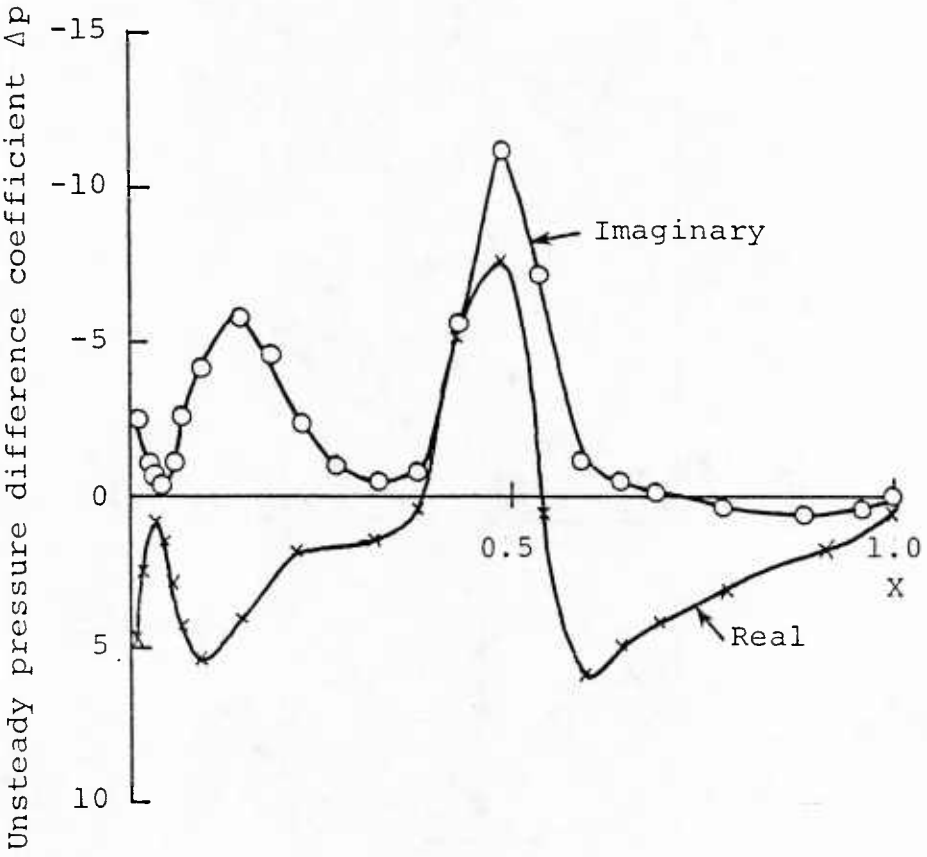

Figure 7.- Unsteady pressure distribution around a supercritical blade cascade in torsion; $M_\infty = 0.707$, $G = 1.372$, $\nu = 1.0$.

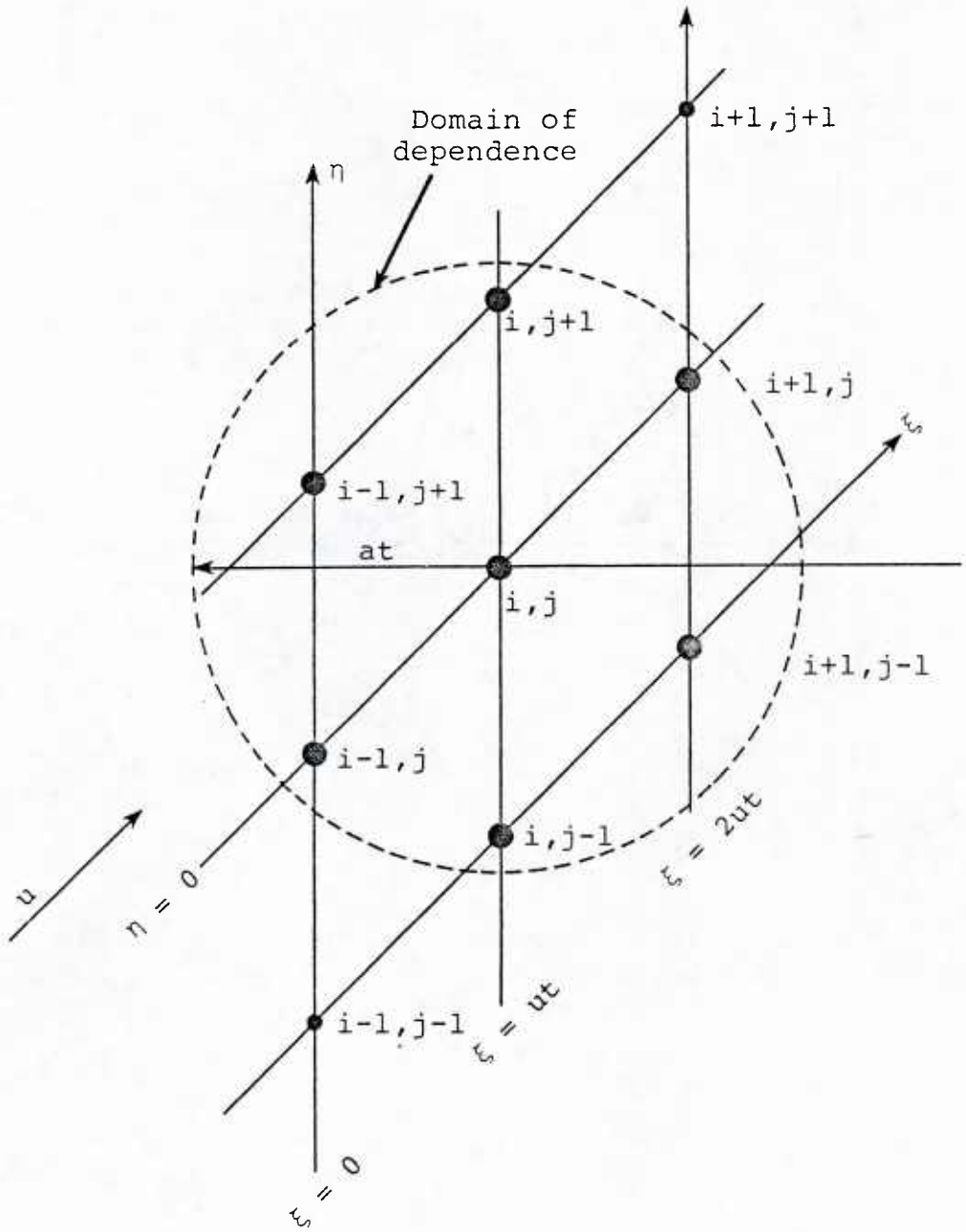

Figure 8.- Schematic of difference cell in a skewed coordinate system.

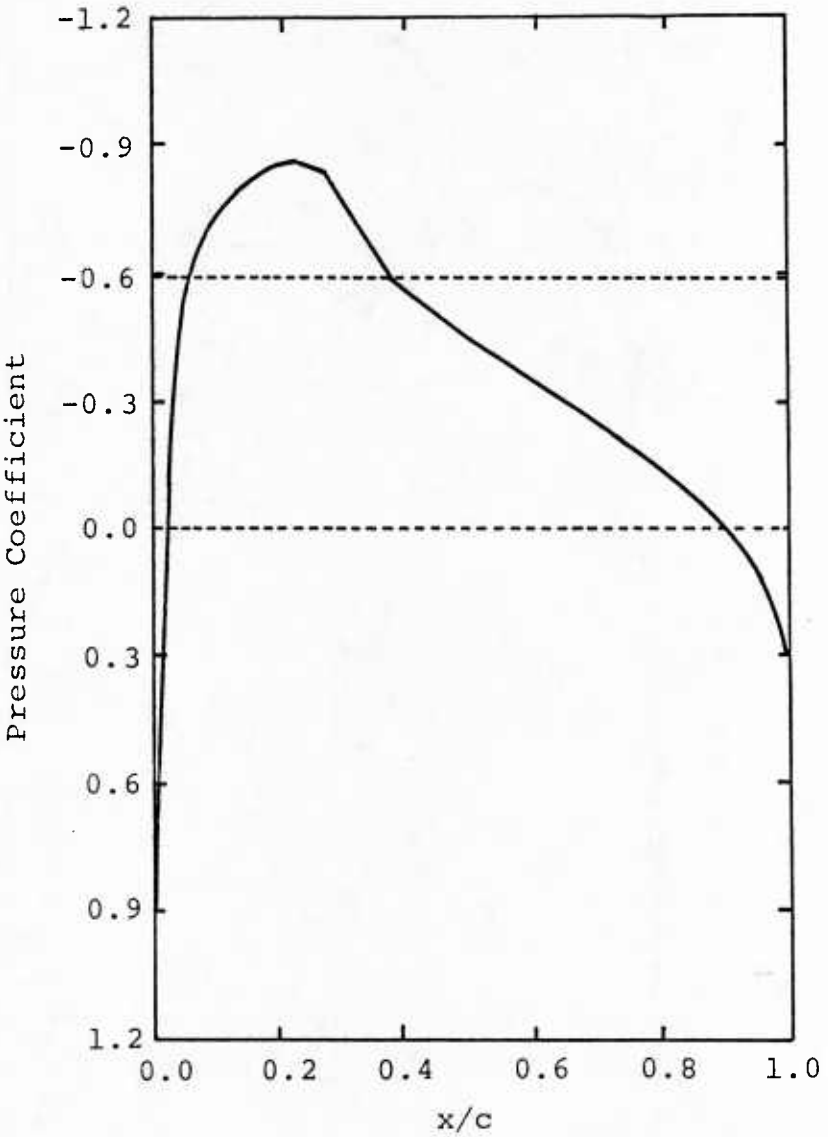

(a) $\theta_s = 0°$

Figure 9.- Steady pressure distribution through a cascade of NACA 0012 sections; $M_\infty = 0.75$, $G = 2$.

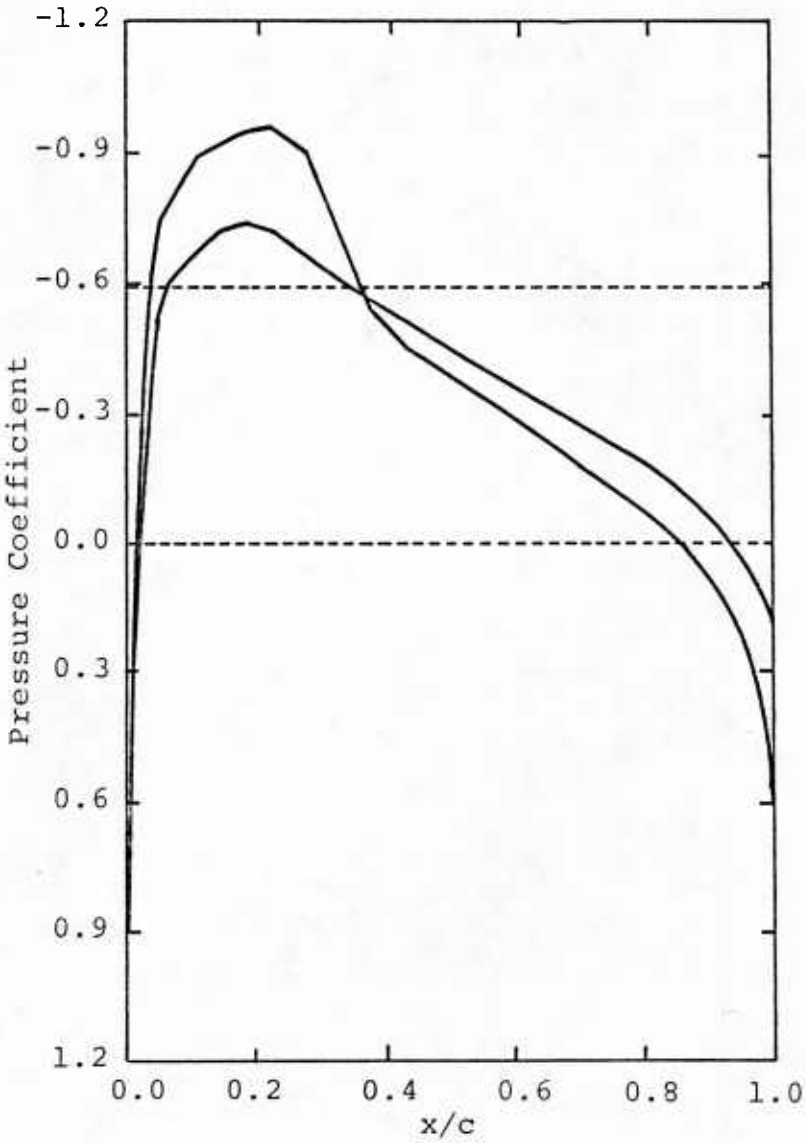

(b) $\theta_s = 15°$

Figure 9.- Continued.

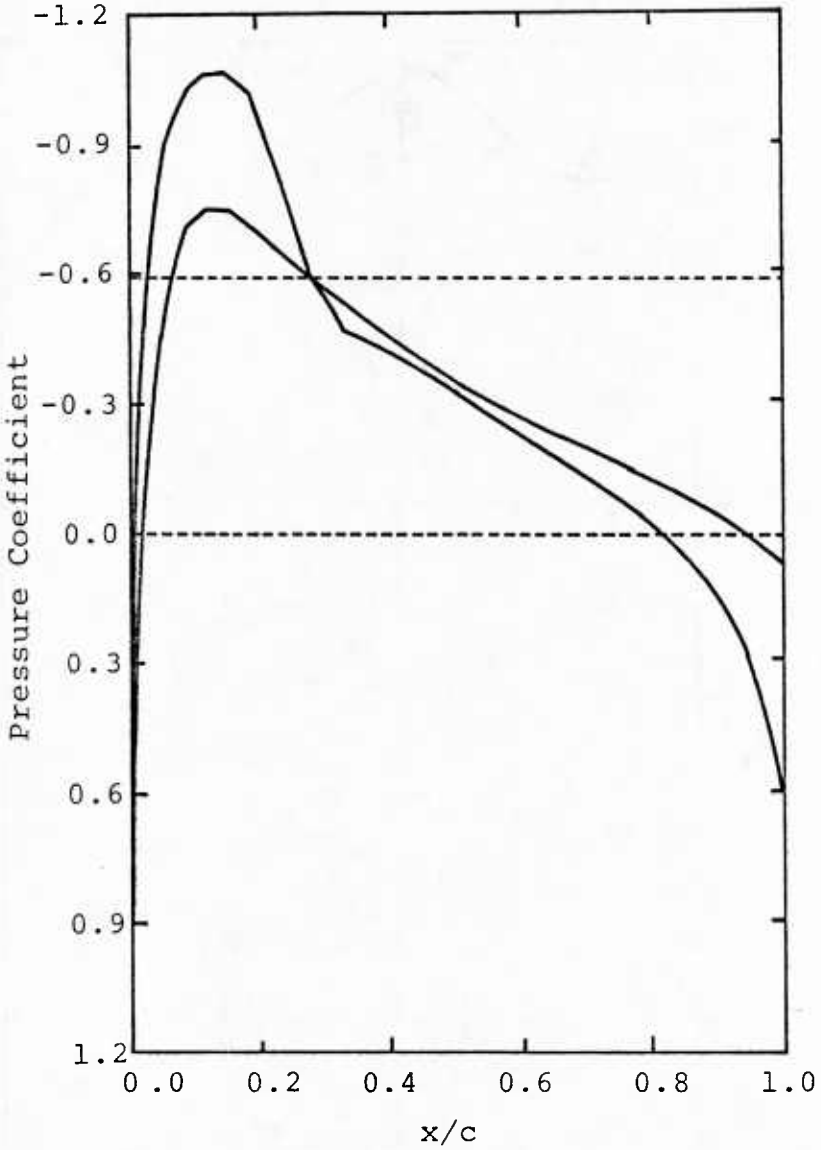

(c) $\theta_s = 45°$

Figure 9.- Concluded.

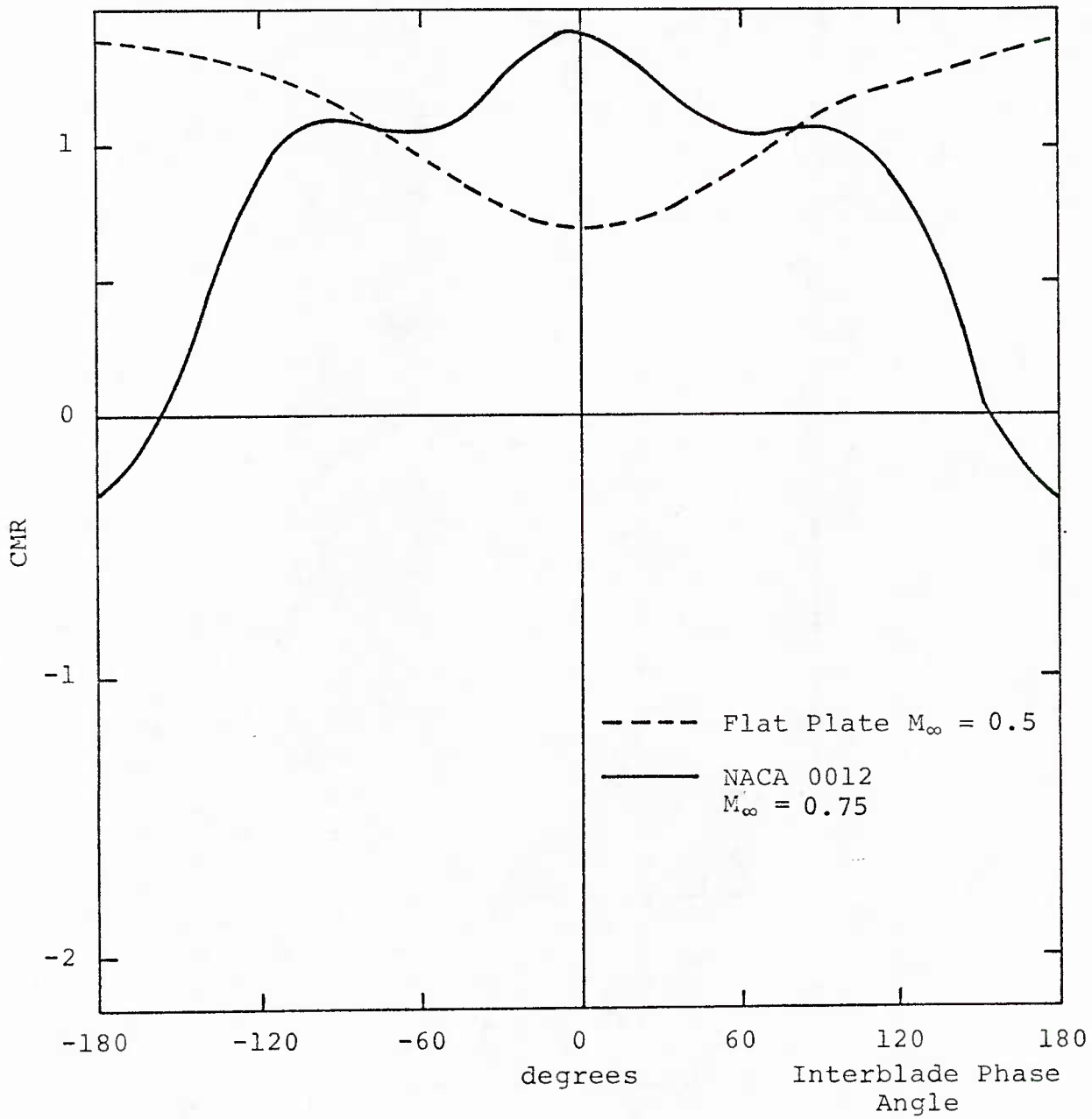

(a) Real part

Figure 10.- Variation of pitching moment with interblade phase angle.

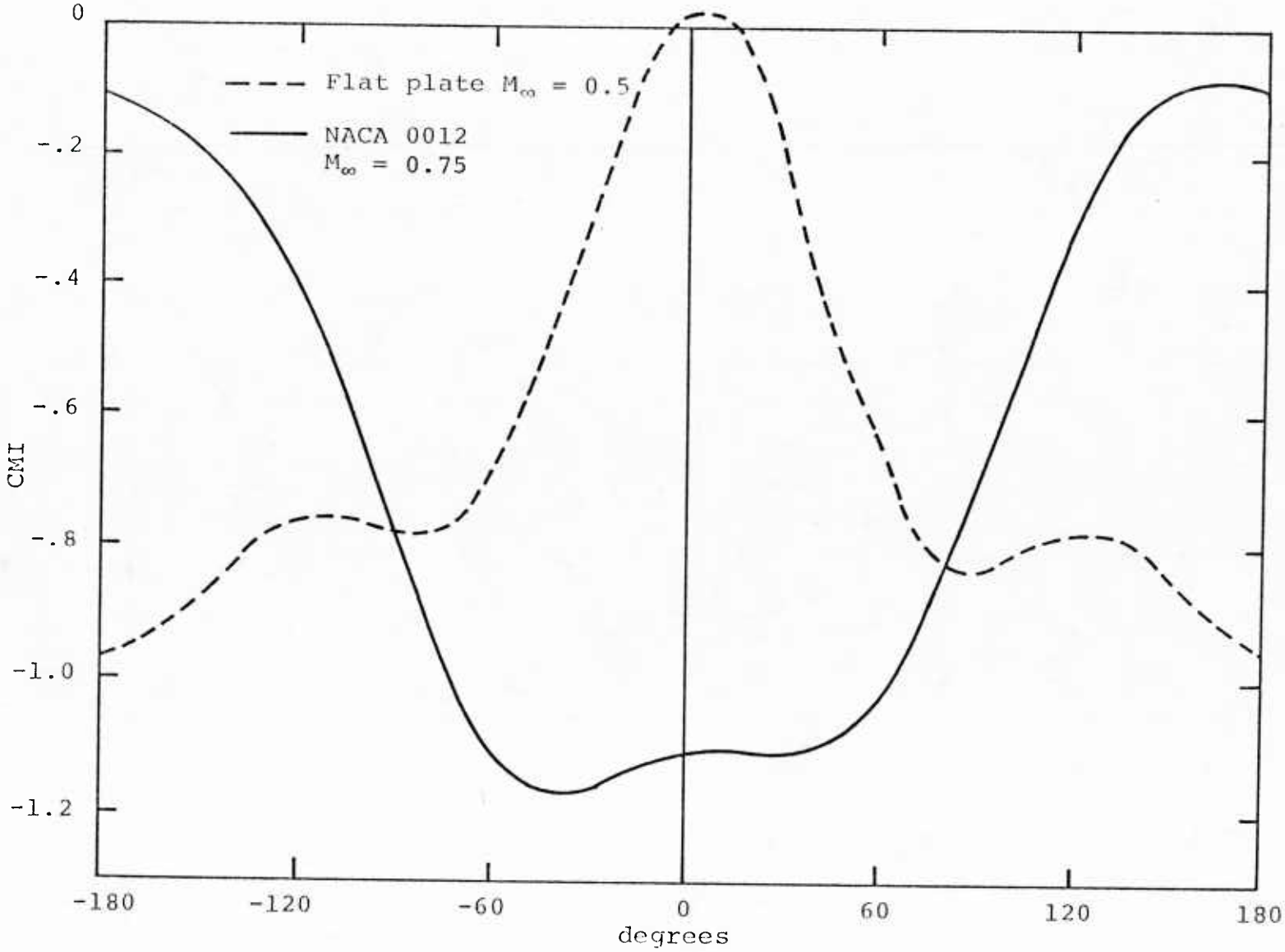

(b) Imaginary part

Figure 10.- Concluded.

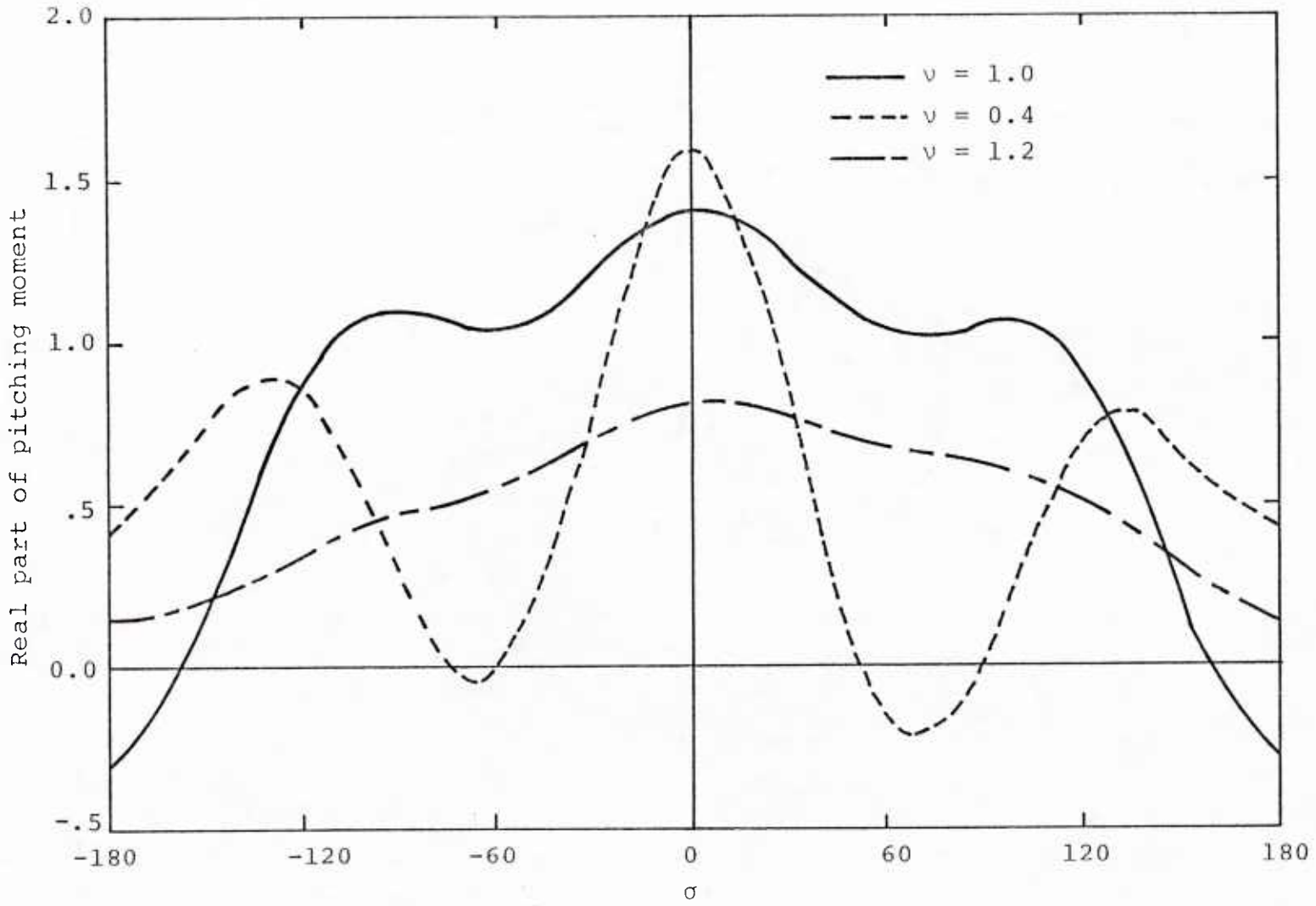

(a) Real part

Figure 11.- Variations of moment coefficients with interblade phase angle and frequency. NACA 0012 section $M_\infty = 0.75$, $G = 2.0$.

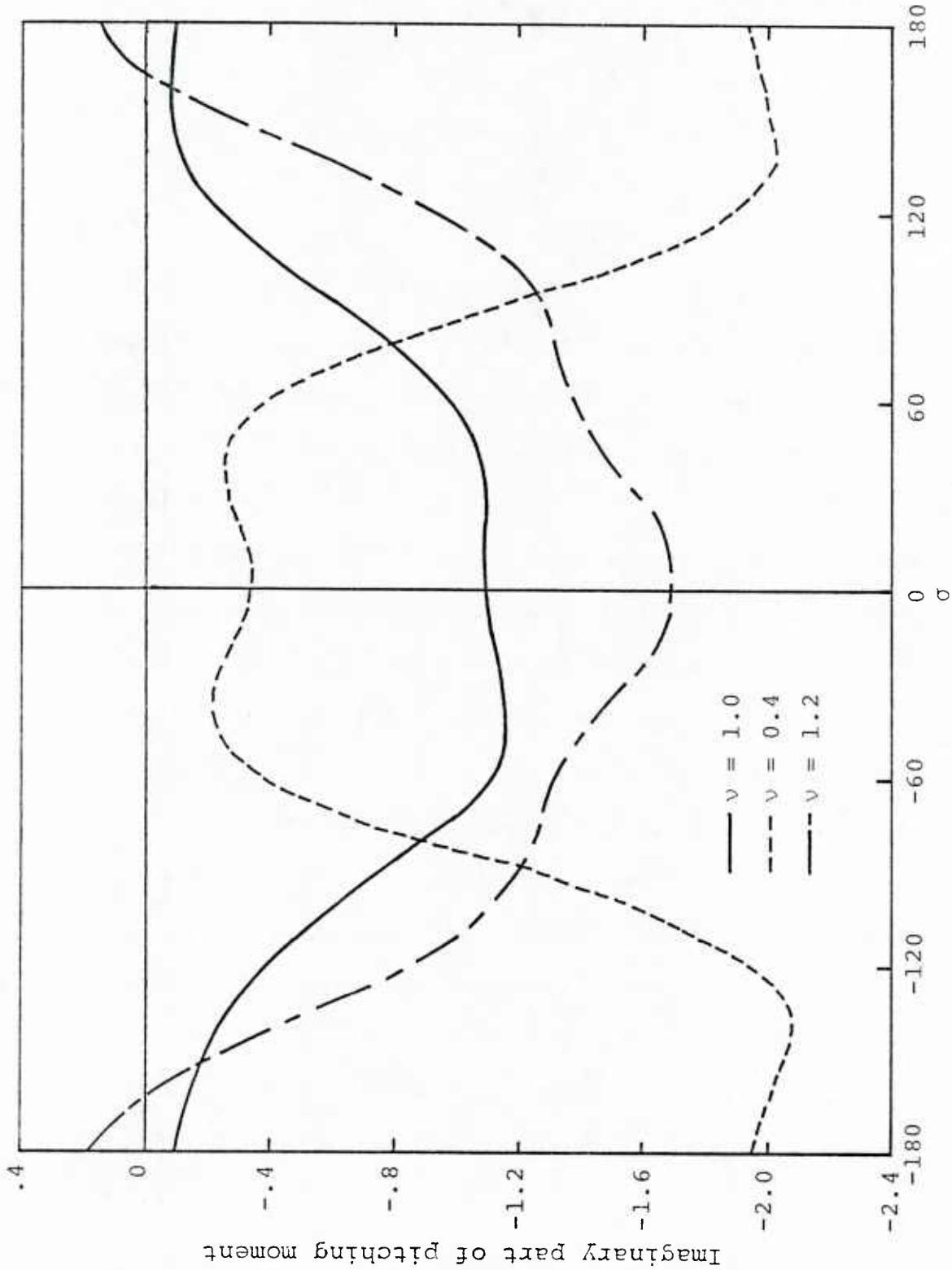

(b) Imaginary part

Figure 11.- Concluded.

APPENDIX

NOTES ON THE COMPUTATIONS OF UNSTEADY TRANSONIC CASCADE FLOWS

David Nixon*

Nielsen Engineering & Research, Inc.

Mountain View, California

INTRODUCTION

In an oscillating cascade there is by definition a fundamental periodicity that occurs every 2N blades (2N is the number of blades in the compressor row). The unsteady flow at each blade will have a periodic boundary condition, as in steady flow, but will lag by a phase angle of $(p/N)\pi$ in relation to the neighboring blade, where p is an integer less than or equal to N whose value is determined as part of the flutter solution. In a nonlinear transonic numerical scheme the choice is between computing the entire 2N blade sequence with the usual periodic boundary conditions at the extremities or to compute the usual three blade cascade problem for each specified value of p. These numerical calculations are computationally expensive and it is desirable to reduce the overall cost of a flutter calculation. Both of these choices involve a large amount of computer time for

*Research Scientist, Associate Fellow AIAA

practical cases, and in case of the first choice, a major development of a computer code. However, it is possible to devise a simpler approach to the problem.

The basic idea of this paper is to devise an elementary problem in which only one blade is in motion, the others being fixed; the motion may be any general time dependent function. This removes the problem of computing the flow for each blade phase angle. This elementary problem is solved for a particular moving blade and the functional form of the velocity potential for both space and time is then known. Because of periodicity in both space and time, these elementary solutions can be superimposed, with reparameterized space and time variables, so that the sum of the solutions satisfies both the basic differential equation and the correct boundary conditions on every blade. Although the most important application of this superposition principle is the development of the correct linearization of the transonic flow equations with discontinuities, these equations are much too complicated for an illustration of the superposition technique. Hence, in the following only a simple, subsonic problem is examined. The general theory is directly extendable to discontinuous transonic flows using the strained coordinate theory of Nixon (ref. 1).

ANALYSIS

Consider the cascade of 2N blades pictured in fig. 1, where blade J+N and blade J-N are identified. The equation for the perturbation velocity potential, $\phi(\bar{x},t)$, due to a time dependent behavior of the blades, will be linear and can be represented as follows:

$$L(\bar{x},t)\phi = 0 \qquad (1)$$

Here, $\bar{x}$ is a general vector coordinate centered on the blade of interest, t is time, and $L(\bar{x},t)$ is a differential operator with variable coefficients. These coefficients arise from the mean steady flow solution about which the flow is perturbed, are functions only of $\bar{x}$, and are periodic in space with period of 2N blades. The time t only occurs through the inclusion of time derivatives. Such an operator occurs in the subsonic flow analysis of Verdon and Caspar (ref. 2) who use the equation

$$\left\{\left[\frac{\partial}{\partial t} + \nabla\Phi \cdot \nabla\right]\left[\frac{\partial}{\partial t} + \nabla\Phi \cdot \nabla\right] + (\gamma - 1)\nabla\Phi\left[\frac{\partial}{\partial t} + \nabla\Phi \cdot \nabla\right]\right.$$

$$\left. + \nabla\left[\frac{\nabla\Phi \cdot \nabla\Phi}{2}\right] \cdot \nabla - a^2\nabla^2\right\}\phi = 0$$

where Φ is the steady state potential. For a staggered cascade the upstream and downstream boundary conditions will depend on the

particular region of the flow that is being considered, for example the far upstream boundary D_{uj} and the far downstream boundary D_{Dj} shown in figure 1. The boundary conditions will depend on the steady far field velocity, which has spatial periodicity and on the phase of the waves produced by the oscillating cascade. Since the individual blade flows are identical except for phase lag of jt_o, it follows that the far field boundary conditions are

$$\phi_u(\bar{x}_u,t) = g_u(\bar{x}_u,t_j) \quad \text{on } D_{uj}, \quad j = -N,N$$
$$\phi_D(\bar{x}_D,t) = g_C(\bar{x}_C,t_j) \quad \text{on } D_{Dj}, \quad j = -N,N \tag{2}$$

where $\bar{x}_u$, $\bar{x}_D$ denote the location of the upstream and downstream boundaries respectively and g_u and g_D are the corresponding spatially asymptotic values of $\phi(\bar{x},t)$. The time t_j is given by $t_j = t - jt_o$ where t_o is the interblade phase lag. The tangential boundary conditions are

$$v_j(\pm\bar{x},t) = f_j(\pm\bar{x},t_j) \quad \text{on } S_j; \quad j = -N,N \tag{3}$$

where v_j is the normal velocity component, f_j is a function of the specified perturbation of blade geometry and S_j denotes the location of the j^{th} blade surface. The $\pm$ signs denote conditions on the upper and lower surface of the blades, respectively. The effect of the interblade phase lag is seen in

equations (2) and (3) where the potentials ϕ_u, ϕ_D or the velocity of the j^{th} blade at time t are given in terms of a function at a time t_j. For blade number 0, periodicity can be applied on $j = \pm N$. In addition to the above boundary conditions the wake condition is

$$\Delta C_p(\bar{x},t) = 0 \text{ on } w_j \tag{4}$$

where ΔC_p is the pressure jump across the wake of the j^{th} blade, w_j, and is a function of $\phi(\bar{x},t)$. Now if the principle of superposition holds then a variable $\phi_j(\bar{x}_j,t)$ can be introduced such that

$$\phi(\bar{x},t) = \sum_{j=-N}^{N} \phi_j(\bar{x}_j,t) \tag{5}$$

where

$$\bar{x}_j = \bar{x} - \tilde{x}_j$$

and $\tilde{x}_j$ is the location of the general coordinate system centered on the j^{th} blade and $x_o \equiv \bar{x}$. Assume that ϕ_j is such that

$$L(\bar{x},t)\phi_j = 0 \tag{6}$$

It is obvious that if equation (6) is used with equation (5) then equation (1) is recovered.

The operator $L(\bar{x},t)$ is a differential operator with coefficients that are functions of the steady

flow over a cascade and hence $L(\bar{x},t)$ is periodic in the spatial dimensions. Thus $L(\bar{x},t)$ is the same no matter on which blade the coordinate system is centered. Hence

$$L(\bar{x},t) = L(\bar{x}_j,t) \tag{7}$$

Furthermore, since t only appears in the operator through a derivative then the variable t can be replaced by t_j. Thus

$$L(\bar{x},t) = L(\bar{x}_j,t_j) \tag{8}$$

Using equations (6) and (8) then gives

$$L(\bar{x}_j,t_j)\phi_j = 0 \tag{9}$$

The next task is to determine suitable boundary conditions. Let

$$\begin{aligned}
&\phi_j(\bar{x}_u,t_j) = g_u(\bar{x}_u,t_j) \quad \text{on } D_{uj} \\
&\phi_j(\bar{x}_D,t_j) = g_D(\bar{x}_D,t_j) \quad \text{on } D_{Dj} \\
&\phi_j(\bar{x}_u,t_j) = 0 \quad \text{on } D_{uk}, \quad k \neq j \\
&\phi_j(x_D,t_j) = 0 \quad \text{on } D_{Dk}, \quad k \neq j
\end{aligned} \tag{10}$$

$$v_j(\pm\bar{x}_j, t_j) = y_s'(\pm\bar{x}_j, t_j) \quad \text{on } S_j$$

$$v_j\left[\pm(\bar{x}_j - \bar{x}_k), t_j\right] = 0 \quad \text{on } S_{j+k} \quad k = 1, N-1$$

$$v_j\left[\pm(\bar{x}_j + \bar{x}_\ell), t_j\right] = 0 \quad \text{on } S_{j-\ell} \quad \ell = 1, N-1 \tag{11}$$

$$\Delta C_{pj}(\bar{x}_j, t_j) = 0 \quad \text{on } w_j$$

where

$$C_p(\bar{x}, t) = \sum_{-N}^{N} C_{pj}(\bar{x}_j, t) \tag{12}$$

It should be noted that in the $(\bar{x}_j, t_j)$ coordinate system each of elementary problems for ϕ_j is identical.

Periodicity is applied in the $j = \pm N$ blades and their wakes. The wake boundary condition is given by

$$\Delta C_{p_j}\left|(\bar{x}_j - \tilde{x}_k), t_j\right| = 0 \quad \text{on } w_{j+k} \quad k = 1, N-1$$

$$\Delta C_{p_j}\left|(\bar{x}_j + x_\ell), t_j\right| = 0 \quad \text{on } w_{j-\ell} \quad \ell = 1, N=1 \tag{13}$$

This is equivalent to keeping all blades stationary except the j^{th} blade and allows the relevant wave transmission through each blade wake. Note that the time is always t_j, the time associated with the j^{th} blade. No interblade phase lag is required at this stage.

When ϕ_j are summed, together with the boundary conditions, the problem defined by equations (5), (10), (11), (12), and (13) is identical to the problem defined by equations (1), (2), (3), and (4). Hence the problem for any time lag t_o between blades can be constructed from the superposition of the elementary problem defined by equations (9), (11), (12), and (13). The superposition mechanism is as follows.

Let the solution to the elementary problem for $j = 0$ be given by $\phi_o(\bar{x},t)$. The solution for $\phi_j(\bar{x},t_j)$ is then given by

$$\phi_j(\bar{x}_j,t_j) = \phi_o(\bar{x},t) \tag{14}$$

Since the functional form of ϕ_o with both $\bar{x}$ and t is known from the elementary solution for $j = 0$ this reparameterization is trivial. The final solution for the zeroth blade is then given by equations (5) and (14); thus

$$\phi(\bar{x},t) = \sum_{-N}^{N} \phi_o(\bar{x} - \tilde{x}_j,\ t - jt_o) \tag{15}$$

Thus the complete time dependent cascade flow for any interblade phase angle can be constructed by superposition of the elementary problem defined by equations (5), (10), (11), (12), and (13).

If $\phi(\bar{x},t)$ and its derivatives are continuous a similar relation to equation (15) can be constructed for the pressure coefficient $C_p(\bar{x},t)$. In addition, similar formulae can be derived for the lift and moment coefficients.

The idea discussed above can be extended to discontinuous transonic flows using the method of strained coordinates (ref. 1). Results are given by Kerlick and Nixon (ref. 3).

CONCLUDING REMARKS

The main contribution to the computation time for an unsteady calculation of cascade flutter in a transonic flow is the need to repeat the calculation for a range of interblade phase angles. The present analysis shows how this problem can be eliminated by a judicious choice of elementary solutions.

REFERENCES

1. Nixon, D.: Notes on the Transonic Indicial Method. AIAA Journal, Vol. 16, No. 6, pp. 613-616, June 1978.

2. Verdon, J.M. and Caspar, J.R.: Subsonic Flow Past an Oscillating Cascade with Finite Mean Flow Deflection. AIAA Journal, Vol. 18, No. 5, 1980.

3. Kerlick, G.D. and Nixon, D.: A High Frequency Transonic Small Disturbance Code for Unsteady Flows in a Cascade. AIAA Paper 82-0955, 1982.

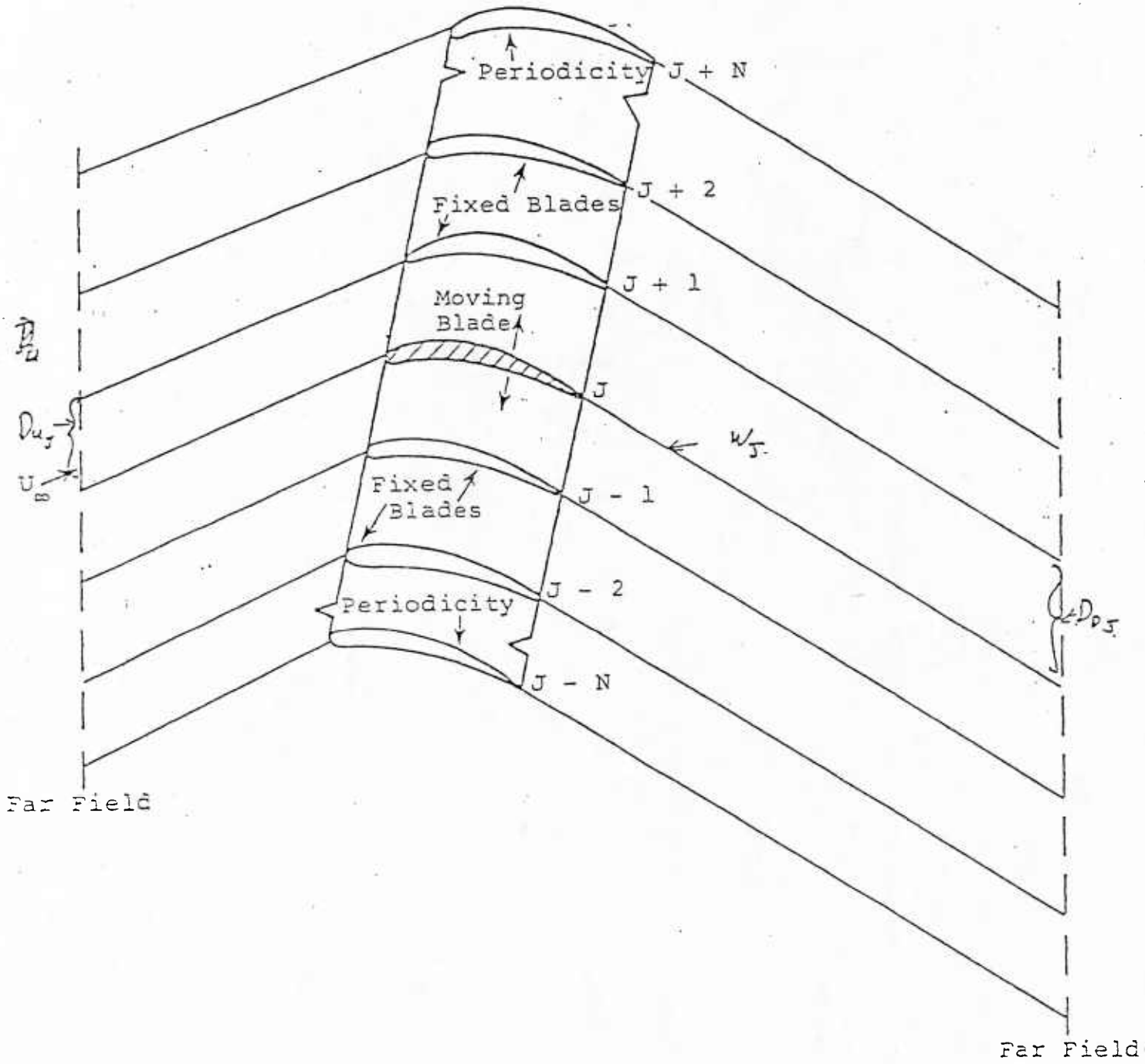

Figure 1.- Sketch of Cascade Problem

DISTRIBUTION LIST FOR UNRESTRICTED REPORTS

1.	Commander Naval Air Systems Command Washington, DC 20361 Attention: Code AIR 310	1
	Code AIR 310E	1
	Code AIR 310F	1
	Code AIR 320D	1
	Code AIR 530	1
	Code AIR 536	1
	Code AIR 7226	4
	Code AIR 03D	1
2.	Office of Naval Research 800 N. Quincy Street Arlington, VA 22217 Attention: Dr. A. D. Wood	2
3.	Commanding Officer Naval Air Propulsion Center Trenton, NJ 08628 Attention: M. Bell	2
4.	Commanding Officer Naval Air Development Center Warminster, PA 19112 Attention: AVTD	1
5.	Library Code 1424 Naval Postgraduate School Monterey, CA 93943	1
6.	Library Army Aviation Material Laboratories Department of the Army Fort Eustis, VA 23604	1
7.	Dr. Arthur J. Wennerstrom AFWAL/POTX Wright-Patterson AFB Dayton, OH 45433	1
8.	Air Force Office of Scientific Research AFOSR/NA Bolling Air Force Base Washington, DC 20332 Attn: Mr. James Wilson	1

9. Chief, Fan and Compressor Branch — 1
Mail Stop 5-9
NASA Lewis Research Center
21000 Brookpark Road
Cleveland, OH 44135

10. National Aeronautics & Space Administration — 1
Lewis Research Center (Library)
21000 Brookpark Road
Cleveland, OH 44135

11. Library — 1
General Electric Company
Aircraft Engine Technology Division
DTO Mail Drop H43
Cincinnati, OH 45215

12. Library — 1
Pratt & Whitney Aircraft Group
Post Office Box 2691
West Palm Beach, FL 33402

13. Library — 1
Pratt-Whitney Aircraft Group
East Hartford, CT 06108

14. Library — 1
Curtis Wright Corporation
Woodridge, NJ 07075

15. Library — 1
AVCO/Lycoming
550 S. Main Street
Stratford, CT 06497

16. Library — 1
Teledyne CAE, Turbine Engines
1330 Laskey Road
Toledo, OH 43612

17. Library — 1
Williams International
Post Office Box 200
Walled Lake, MI 48088

18. Library — 1
Detroit Diesel Allison Division G.M.C.
Post Office Box 894
Indianapolis, IN 46202

19. Library 1
Garrett Turbine Engine Company
111 S. 34th Street
Post Office Box 5217
Phoenix, AZ 85010

20. Turbopropulsion Laboratory 5
Code 67Sf
Naval Postgraduate School
Monterey, CA 93943